Measuring flow resistivity of porous material via acoustic reflected waves

Naima Sebaa, Zine El Abiddine E.A. Fellah, Mohamed Fellah, Walter Lauriks, Claude Depollier

Measuring flow resistivity of porous material via acoustic reflected waves

N. Sebaa
Laboratorium voor Akoestiek en Thermische Fysica, Katholieke Universiteit Leuven, Celestijnenlaan 200 D, B-3001 Heverlee, Belgium

Z. E. A. Fellah[a)]
Laboratoire de Mécanique et d'Acoustique, Centre National de la Recherche Scientifique (CNRS)-UPR 7051, 31 Chemin Joseph Aiguier, Marseille 13402, France

M. Fellah
Laboratoire de Physique Théorique, Institut de Physique, Université des Sciences et de la Technologie Houari Boumedie (USTHB), BP 32 El Alia, Bab Ezzouar 16111, Algeria

W. Lauriks
Laboratorium voor Akoestiek en Thermische Fysica, Katholieke Universiteit Leuven, Celestijnenlaan 200 D, B-3001 Heverlee, Belgium

C. Depollier
Laboratoire d'Acoustique de l'Université du Maine, Unité Mixte de Recherche-Centre National de la Recherche Scientifique (UMR-CNRS) 6613, Université du Maine, Avenue Olivier Messiaen, 72085 Le Mans Cedex 09, France

(Received 9 March 2005; accepted 2 September 2005; published online 18 October 2005)

An acoustic reflectivity method is proposed for measuring flow resistivity of porous materials having rigid frame. The flow resistivity of porous material is defined as the ratio between the pressure difference across a sample and the velocity of flow of air through that sample per unit cube. It is important as one of the several parameters required by acoustical theory to characterize porous materials like plastic foams and fibrous or granular materials. The proposed method is based on a temporal model of the direct and inverse scattering problem for the diffusion of transient low-frequency waves in a homogeneous isotropic slab of porous material having a rigid frame. This time domain model of wave propagation was initially introduced by the authors [Z.E.A. Fellah and C. Depollier, J. Acoust. Soc. Am. **107**, 683 (2000)]. The viscous losses of the medium are described by the model devised by Johnson *et al.* [D. L. Johnson, J. Koplik, and R. Dashen, J. Fluid. Mech. **176**, 379 (1987)]. Reflection and transmission scattering operators for a slab of porous material are derived from the responses of the medium to an incident acoustic pulse. The flow resistivity is determined from the expression of the reflection operator. Experimental and numerical validation results of this method are presented. A guide (pipe) is used in the experiment for obtaining a plane wave. This method has the advantage of being simple, rapid, and efficient. © *2005 American Institute of Physics*. [DOI: 10.1063/1.2099510]

I. INTRODUCTION

The propagation of sound in fluid-saturated porous media with rigid solid frames is of great interest for a wide range of industrial applications. With air as the pore fluid,[1–5] applications can be found in noise control, nondestructive material characterization, thermoacoustically controlled heat transfer, etc.

The determination of the properties of a medium using waves that have been reflected by or transmitted through the medium is a classical inverse scattering problem.[6,7] Such problems are often approached by taking a physical model of the scattering process, generating a synthetic response for a number of assumed values for the parameters, and adjusting these parameters until a reasonable level of correspondence is attained between the synthetic response and the data observed.

One important parameter which appears in theories of sound propagation in porous materials at low-frequency range[3] is the flow resistivity. This parameter intervenes in the description of the viscous coupling between the fluid and the structure. As such, in studies of acoustical properties of porous materials, it is extremely useful to be able to measure this parameter. The flow resistance[8–16] of porous material is defined as the ratio between the pressure difference across a sample and the velocity of flow of air through that sample; the flows being considered are steady and nonpulsating. This is quite analogous to the definition of electrical resistance as the ratio between voltage drop and current. The flow resistivity σ of a porous material is defined as the flow resistance per unit cube.

Many methods have been proposed in the past in the fluid mechanics field, developing instrumentation to measure accurately various properties of fluids.[17] Systems for the measurement of flow resistance are largely based on this technology, making use of techniques for measuring flow rates of fluids and pressure differences.

[a)]Electronic mail: fellah@lma.cnrs-mrs.fr

Among the various systems that have been developed for the measurement of flow resistance, a distinction can be made between direct and comparative methods. With direct methods, the pressure drop across a sample and the rate of air flow through the porous sample are determined separately and the flow resistance is computed as the ratio of the two quantities. One example of this type of system has been given by Morse *et al.*[14] and Brown and Bolt.[11] Air is drawn into a container after passing through a sample. Pressure differences are measured across the sample using a water nanometer, and air flows are obtained from the rate at which water siphons out of the container. Leonard[12] adapted an analytical beam balance to enable small pressure differences to be measured with considerably improved resolution. This technique, because of its simplicity and accuracy, is now widely used for the measurement of flow resistance. Bies and Hansen[9] have improved upon the configuration of Morse *et al.*[14] using a "barocell" and digital nanometer to make precise measurements of pressure differences.

With comparative methods, a calibrated flow resistance is placed in series with the porous sample. The ratio of pressure drops across each element is the same as the ratio of the values of flow resistance, since the volumetric flow of air in the line is constant. This method has been developed by Gemant,[18] in which capillary tubes have been used as known flow resistances. Stinson and Daigle[13] have used a laminar flow element as known flow resistance.

In this work, we present a simple acoustical method of measuring specific flow resistivity by measuring a diffusive wave reflected by a slab of porous material having a high porosity in a guide (pipe). The guide (pipe) is used in the experiment for obtaining a plane wave. This method is based on a temporal model of the direct and inverse scattering problem for the diffusion of transient low-frequency waves in a homogeneous isotropic slab of porous material having a rigid frame. This work was initially introduced by the authors of Ref. 3. The viscous and thermal losses of the medium are described by the models of Johnson *et al.*[19] and Allard[1] used in the time domain. Reflection and transmission scattering operators of a slab of porous material are derived and thus the responses of the medium to an incident acoustic pulse are obtained.

The outline of this work is as follows. Section II recalls a time domain model and the basic equations of wave diffusion in porous material. Section III is devoted to the direct problem and to the expression of the reflection scattering operator in the time domain. In Sec. IV, the sensitivity of the porosity and the specific flow resistivity are discussed, showing the effect of each parameter on the reflected wave by the porous slab. Section V deals with the inverse problem and the appropriate procedure, based on the least-square method, which is used to estimate the specific flow resistivity. Finally in Sec. VI, experimental validation using low-frequency acoustic measurement is discussed for air-saturated industrial plastic foams.

II. POROUS MATERIALS HAVING A RIGID FRAME

In the acoustics of porous materials, one distinguishes two situations according to whether the frame is moving or not. In the first case, the dynamics of the waves due to the coupling between the solid skeleton and the fluid is well described by the Biot theory.[20] In air-saturated porous media, the structure is generally motionless and the waves propagate only in fluid. This case is described by the model of equivalent[21] fluid which is a particular case of the Biot model.

A. Equivalent fluid model

Let a homogeneous isotropic porous material with porosity ϕ be saturated with a compressible and viscous fluid of density ρ and viscosity η. It is assumed that the frame of this porous solid is not deformable when it is subjected to an acoustic wave. It is the case, for example, for a porous medium which has a large skeleton density or very large elastic modulus or weak fluid-structure coupling. To apply the results of continuum mechanics it is required that the wavelength of sound should be much larger than the sizes of the pores or grains in the medium. In such a porous material, acoustic waves propagate only in the fluid so, it can be seen as an equivalent fluid, the density and the bulk modulus of which are "renormalized" by the fluid-structure interactions. A prediction of the acoustic comportment of the porous material requires the determination of the dynamic tortuosity $\alpha(\omega)$ and the dynamic compressibility $\beta(\omega)$. These functions depend on the physical characteristics of the fluid in the pore space of the medium and are independent of the dynamic characteristics of the structure. The basic equations of the model of equivalent fluid are

$$\rho\alpha(\omega)i\omega v_i = -\nabla_i p, \quad i\frac{\beta(\omega)}{K_a}p = -\nabla\cdot\mathbf{v}. \tag{1}$$

In these relations, v and p are the particle velocity and the acoustic pressure and K_a is the compressibility modulus of the fluid. The first equation is the Euler equation, and the second one is a constitutive equation obtained from the equation of mass conservation associated with the behavior (or adiabatic) equation. $\alpha(\omega)$ and $\beta(\omega)$ are the dynamic tortuosity of the medium and the dynamic compressibility of the air included in the porous material. These two factors are complex functions which heavily depend on the frequency $f = \omega/2\pi$. Their theoretical expressions are given by Johnson *et al.*,[19] Allard,[1] and Lafarge *et al.*,[22]

$$\alpha(\omega) = \alpha_\infty\left(1 + \frac{\phi\sigma}{i\omega\alpha_\infty\rho_f}\sqrt{1 + i\frac{4\alpha_\infty^2\eta\rho_f\omega}{\sigma^2\Lambda^2\phi^2}}\right), \tag{2}$$

$$\beta(\omega) = \gamma - (\gamma-1)\left(1 + \frac{\eta\phi}{i\omega\rho_f k_0' P_r}\sqrt{1 + i\frac{4k_0'^2\rho_f\omega P_r}{\eta\phi^2\Lambda'^2}}\right)^{-1}, \tag{3}$$

where $i^2=-1$, γ represents the adiabatic constant, P_r the Prandtl number, α_∞ the tortuosity, σ the flow resistivity, k_0' the thermal permeability,[22] and Λ and Λ' the viscous and thermal characteristic lengths.[1,19] This model was initially developed by Johnson *et al.*[19] and completed by Allard[1] by adding the description of thermal effects. Later on, Lafarge *et al.*[22] introduced the parameter k_0' which describes the additional damping of sound waves due to the thermal exchanges

between fluid and structure at the surface of the pores.

The functions $\alpha(\omega)$ and $\beta(\omega)$ express the viscous and thermal exchanges between the air and the structure which are responsible for the sound damping in acoustic materials. These exchanges are due on the one hand to the fluid-structure relative motion and on the other hand to the air compression dilatations produced by the wave motion. The parts of the fluid affected by these exchanges can be estimated by the ratio of a microscopic characteristic length of the media, as, for example, the sizes of the pores, to the viscous and thermal skin depth thickness $\delta=(2\eta/\omega\rho_0)^{1/2}$ and $\delta'=(2\eta/\omega\rho_0 P_r)^{1/2}$. For the viscous effects this domain corresponds to the region of the fluid in which the velocity distribution is perturbed by the frictional forces at the interface between the viscous fluid and motionless structure. For the thermal effects, it corresponds to the fluid volume affected by the heat exchange between the two phases of the porous medium. In this model, the sound propagation is completely determined by the six following parameters: ϕ, α_∞, σ, k_0', Λ, and Λ'.

B. Viscous domain

In this domain, the viscous forces are important everywhere in the fluid, the compression-dilatation cycle in the porous material is slow enough to favor the thermal exchange between fluid and structure. At the same time the temperature of the frame is practically unchanged by the passage of the sound wave because of the high value of its specific heat: the frame acts as a thermostat. In this case the isothermal compressibility is directly applicable. This domain corresponds to the range of frequencies such that viscous skin thickness $\delta=(2\eta/\omega\rho_0)^{1/2}$ is much larger than the radius of the pores r,

$$\frac{\delta}{r} \gg 1. \tag{4}$$

This is called the low-frequency range. For these frequencies, We consider the low-frequency approximations of the response factor $\alpha(\omega)$ and $\beta(\omega)$. When $\omega \to 0$, Eqs. (2) and (3), respectively, become

$$\alpha(\omega) = \frac{\sigma\phi}{i\omega\rho}, \tag{5}$$

$$\beta(\omega) = \gamma. \tag{6}$$

For a wave traveling along the direction x, the generalized forms of the basic equations (1) in the time domain are now

$$\sigma\phi V = -\frac{\partial p}{\partial x} \text{ and } \frac{\gamma}{K_a}\frac{\partial p}{\partial t} = -\frac{\partial v}{\partial x}, \tag{7}$$

where the Euler equation is reduced to Darcy's law which defines the static flow resistivity $\sigma=\eta/k_0$. The wave equation in time domain is given by

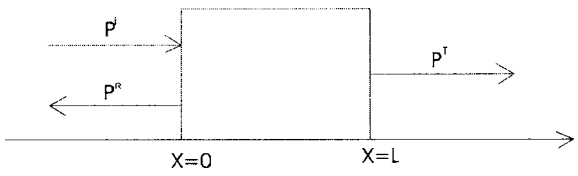

FIG. 1. Geometry of the problem.

$$\frac{\partial^2 p}{\partial x^2} + \left(\frac{\sigma\phi\gamma}{K_a}\right)\frac{\partial p}{\partial t} = 0. \tag{8}$$

The fields which are varying in time, the pressure, the acoustic velocity, etc., follow a diffusion equation with the diffusion constant

$$D = \frac{K_a}{\sigma\phi\gamma}. \tag{9}$$

A quite similar result is given by Jonhson.[23] However, the adiabatic constant γ does not appear in Johnson's model in which the thermal expansion is neglected. The diffusion constant D is connected to Darcy's constant k_0 (called also the viscous permeability) by the relation

$$D = \frac{K_a k_0}{\eta\phi\gamma}, \tag{10}$$

where η the fluid viscosity.

III. DIRECT PROBLEM

The direct scattering problem is that of determining the scattered field as well as the internal field, that arises when a known incident field impinges on the porous material with known physical properties.

In this section some notation is introduced. The problem geometry is given in Fig. 1. A homogeneous porous material occupies the region $0 \leqslant x \leqslant L$. This medium is assumed to be isotropic and to have a rigid frame. A short sound pulse impinges normally on the medium from the left. It generates an acoustic pressure field $p(x,t)$ and an acoustic velocity field $v(x,t)$ within the material, which satisfy Eq. (8).

To derive the reflection and transmission scattering operators, it is assumed that the pressure field and flow velocity are continuous at the material boundary.

$$\begin{aligned} &p(0^+,t) = p(0^-,t), \quad p(L^-,t) = p(L^+,t), \\ &v(0^-,t) = \phi v(0^+,t), \quad v(L^+,t) = \phi v(L^-,t), \end{aligned} \tag{11}$$

where ϕ is the porosity of the medium and $\pm$ superscript denotes the limit from left and right, respectively. Assumed initial conditions are

$$p\,(x,t)|_{t=0} = 0 \text{ and } \left.\frac{\partial p}{\partial t}\right|_{t=0} = 0, \tag{12}$$

which means that the medium is idle for $t=0$.

If the incident sound wave is generated in the region $x \leqslant 0$, then the expression of the acoustic field in the region to the left of the material is the sum of the incident and reflected fields,

$$p_1(x,t) = p^i\left(t - \frac{x}{c_0}\right) + p^r\left(t + \frac{x}{c_0}\right), \quad x < 0. \tag{13}$$

Here, $p_1(x,t)$ is the field in the region $x<0$ and p^i and p^r denotes the incident and reflected fields respectively. In addition, a transmitted field is produced in the region to the right of the material. This has the form

$$p_3(x,t) = p^t\left[t - \frac{(x-L)}{c_0}\right], \quad x > L. \tag{14}$$

($p_3(x,t)$ is the field in the region $x>L$ and p^t is the transmitted field.)

The incident and scattered fields are related by scattering operators (i.e., reflection and transmission operators) for the material. These are integral operators represented by

$$p^r(x,t) = \int_0^t \tilde{R}(\tau)p^i\left(t - \tau + \frac{x}{c_0}\right)d\tau = \tilde{R}(t) * p^i(t) * \delta\left(t + \frac{x}{c_0}\right), \tag{15}$$

$$p^t(x,t) = \int_0^t \tilde{T}(\tau)p^i\left[t - \tau - \frac{(x-L)}{c_0}\right]d\tau = \tilde{T}(t) * p^i(t) * \delta\left[t - \frac{(x-L)}{c_0}\right]. \tag{16}$$

In Eqs. (15) and (16) functions $\tilde{R}$ and $\tilde{T}$ are the reflection and transmission kernels, respectively, for incidence from the left. Note that the lower limit of integration in (15) and (16) is given as 0, which is equivalent to assuming that the incident wave front first impinges on the material at $t=0$. The operators $\tilde{R}$ and $\tilde{T}$ are independent of the incident field used in the scattering experiment and depend only on the properties of the materials.

Equation (8) is solved by the Laplace transform method by taking into account the conditions (11) and (12). We note $P(x,z)$ the Laplace transform of $p(x,t)$ defined by

$$P(x,z) = \mathcal{L}[p(x,t)] = \int_0^\infty \exp(-zt)p(x,t)dt. \tag{17}$$

Using the following relations:

$$\mathcal{L}[\delta(t)] = 1 \quad \text{and} \quad \mathcal{L}[H(t)] = \frac{1}{z}, \tag{18}$$

the Laplace transform of the diffusive equation (8) satisfying the initials conditions (12) becomes

$$\frac{\partial^2 P_2(x,z)}{\partial x^2} - DzP_2(x,z) = 0, \tag{19}$$

where $P_2(x,z)$ is the Laplace transform of the acoustic pressure $p_2(x,t)$ inside the porous material for $0 \leqslant x \leqslant L$.

The Laplace transform of the field outside the materials is given by

$$P_1(x,z) = \left[\exp\left(-z\frac{x}{c_0}\right) + R(z)\exp\left(z\frac{x}{c_0}\right)\right]\varphi(z), \quad x \leqslant 0, \tag{20}$$

$$P_3(x,z) = T(z)\exp\left[-\frac{(x-L)}{c_0}z\right]\varphi(z), \quad x \geqslant L. \tag{21}$$

Here $P_1(x,z)$ and $P_3(x,z)$ are, respectively, the Laplace transforms, of the field at the left and the right sides of the material, $\varphi(z)$ denotes the Laplace transform of the incident field $p^i(t)$, and finally $R(z)$ and $T(z)$ are the Laplace transforms of the reflection and transmission kernels, respectively.

The Laplace transform of the continuous conditions (11) are written as

$$P_2(0^+,z) = P_1(0^-,z) \quad \text{and} \quad P_2(L^-,z) = P_3(L^+,z), \tag{22}$$

where $P_1(0^-,z)$ and $P_3(L^+,z)$ are the Laplace transforms of $p_1(x,t)$ and $p_3(x,t)$, respectively, given by

$$P_1(0^-,z) = [1 - R(z)]\varphi(z) \quad \text{and} \quad P_3(L^-,z) = T(z)\varphi(z). \tag{23}$$

To derive the reflection and transmission coefficients the boundary-condition flow velocity at the interfaces $x=0$ and $x=L$ are needed.

The equation of the flow continuity at $x=0$ is written as

$$v_1(x,t) = \phi v_2(x,t), \tag{24}$$

where ϕ is the porosity of the medium.

The Euler equation is written in the regions (1) ($x \leqslant 0$) and (2) ($0 \leqslant x \leqslant L$) as

$$\rho_f \left.\frac{\partial v_1(x,t)}{\partial t}\right|_{x=0} = -\left.\frac{\partial p_1(x,t)}{\partial x}\right|_{x=0}, \quad x \leqslant 0, \tag{25}$$

$$\rho_f \tilde{\alpha}(t) * \left.\frac{\partial v_2(x,t)}{\partial t}\right|_{x=0} = -\left.\frac{\partial p_2(x,t)}{\partial x}\right|_{x=0}, \quad 0 \leqslant x \leqslant L, \tag{26}$$

where $v_1(x,t)$ and $v_2(x,t)$ are the acoustic velocity field in the regions (1) and (2), respectively. In the free space [region (1)], the tortuosity operator is equal to 1. From (24), (25), and (26) it is easy to write

$$\tilde{\alpha}(t) * \left.\frac{\partial p_1(x,t)}{\partial x}\right|_{x=0} = \phi \left.\frac{\partial p_2(x,t)}{\partial x}\right|_{x=0}, \tag{27}$$

with

$$\left.\frac{\partial p_1(x,t)}{\partial x}\right|_{x=0} = \frac{1}{c_0}[-\delta(t) + \tilde{R}(t)] * \frac{\partial p^i(t)}{\partial t}. \tag{28}$$

The Laplace transform of Eq. (27) gives a relation between the reflection and transmission coefficients,

$$[R(z) - 1]\sinh(L\sqrt{Dz}) = \phi\rho_0 c_0 \frac{\sqrt{Dz}}{z\alpha(z)}\{T(z) - [1 + R(z)]\cosh(L\sqrt{Dz})\}, \tag{29}$$

where $\alpha(z)$ is the Laplace transform of $\tilde{\alpha}(t)$.

At the interface $x=L$, the continuity of the flow velocity leads to the relation

$$v_3(L^+,t)=\phi v_2(L^-,t). \tag{30}$$

At $x=L$, the Euler equation is written in the two regions (2) and (3) ($x\geqslant L$) as

$$\rho_f \tilde{\alpha}(t) * \left.\frac{\partial v_2(x,t)}{\partial t}\right|_{x=L^-} = -\left.\frac{\partial p_2(x,t)}{\partial t}\right|_{x=L^-},$$
$$\rho_f \left.\frac{\partial v_3(x,t)}{\partial t}\right|_{x=L^+} = -\left.\frac{\partial p_3(x,t)}{\partial x}\right|_{x=L^+}. \tag{31}$$

From Eqs. (30) and (31), we have

$$\tilde{\alpha}(t) * \left.\frac{\partial p_3(x,t)}{\partial x}\right|_{x=L^+} = \phi \left.\frac{\partial p_2(x,t)}{\partial x}\right|_{x=L^-}, \tag{32}$$

with

$$\left.\frac{\partial p_3(x,t)}{\partial x}\right|_{x=L^+} = -\frac{1}{c_0}\tilde{T}(t) * \left.\frac{\partial p^i}{\partial t}\right|_{t=L/c_0}, \tag{33}$$

the Laplace transform of Eq. (32) gives

$$T(z)\sinh(L\sqrt{Dz}) = \phi\rho_0 c_0 \frac{\sqrt{Dz}}{z\alpha(z)}[1+R(z) - T(z)\cosh(L\sqrt{Dz})]. \tag{34}$$

By putting

$$B=\frac{\phi\rho_0 c_0\sqrt{D}}{z\alpha(z)}=\sqrt{\frac{\rho_0^3\phi\gamma}{\eta k_0}}. \tag{35}$$

The reflection and transmission coefficients are the solutions of the system of equations [Eqs. (29) and (34)],

$$R(z)[\sinh(L/\sqrt{Dz})+B\sqrt{z}\cosh(L\sqrt{Dz})]-B\sqrt{z}T(z) = \sinh(L\sqrt{Dz})-B\sqrt{z}\cosh(L\sqrt{Dz}),$$
$$-R(z)B\sqrt{z}+T(z)[\sinh(L\sqrt{Dz})+B\sqrt{z}\cosh(L\sqrt{Dz})]=B\sqrt{z}. \tag{36}$$

$R(z)$ is given by

$$R(z)=\frac{(1-B^2z)\sinh(L\sqrt{Dz})}{2B\sqrt{z}\cosh(L\sqrt{Dz})+(1+B^2z)\sinh(L\sqrt{Dz})}. \tag{37}$$

The development of these expressions in exponential series (Appendix) leads to the reflection coefficient,

$$R(z)=\frac{1-B\sqrt{z}}{1+B\sqrt{z}}\sum_{n\geqslant 0}\left(\frac{1-B\sqrt{z}}{1+B\sqrt{z}}\right)^{2n}\{\exp(-2nL\sqrt{Dz}) - \exp[-2(n+1)L\sqrt{Dz}]\}. \tag{38}$$

These expressions take into account the multiple reflections in the material.

In most cases, in porous materials saturated by air, the multiple reflection effects are negligible because of the high attenuation of sound waves in these media. So, by taking into account only the first reflections at the interfaces $x=0$ and $x=L$, the reflection coefficient in the material becomes

$$R(z)=\frac{1-B\sqrt{z}}{1+B\sqrt{z}}\left[1-\frac{4B\sqrt{z}}{(1+B\sqrt{z})^2}\exp(-2L\sqrt{Dz})\right] = \frac{1-B\sqrt{z}}{1+B\sqrt{z}}-\frac{4B\sqrt{z}(1-B\sqrt{z})}{(1+B\sqrt{z})^3}\exp(-2L\sqrt{Dz}). \tag{39}$$

The reflection scattering operator is calculated by taking the inverse Laplace transform of the reflection coefficient.

We infer[24] that

$$\mathcal{L}^{-1}\left[\frac{1-B\sqrt{z}}{(1+B\sqrt{z})}\right]=\mathcal{L}^{-1}\left[-1+\frac{2}{B}\frac{1}{\sqrt{z}+1/B}\right]=-\delta(t)+\frac{2}{B\sqrt{\pi t}} - \frac{2}{B^2}\exp(t/B^2)\mathrm{erf}(\sqrt{t}/B), \tag{40}$$

where erf is the error function.[24]

By putting

$$g(z)=\frac{Bz-1}{(1+Bz)^3}=\frac{1}{B^2}\frac{z-1/B}{(1/B+z)^3},$$

we obtain

$$\mathcal{L}^{-1}[g(z)]=f(t)=\frac{1}{B^2}\mathcal{L}^{-1}\left[\frac{z-1/B}{(1/B+z)^3}\right] = \frac{1}{B^2}(t-t^2/B)\exp(-t/B).$$

Using the relation

$$\mathcal{L}^{-1}[\sqrt{z}g(\sqrt{z})]=\frac{1}{2\sqrt{\pi}}\frac{1}{t^{3/2}}\int_0^\infty \exp\left(-\frac{u^2}{4t}\right)\left(\frac{u^2}{2t}-1\right)f(u)du = \frac{1}{2\sqrt{\pi}B^2}\frac{1}{t^{3/2}}\int_0^\infty \exp\left(-\frac{u^2}{4t}\right)\left(\frac{u^2}{2t}-1\right) \times\left(u-\frac{u^2}{B}\right)\exp\left(-\frac{u}{B}\right)du,$$

which, with the variable change $u/B=y$, yields

$$\mathcal{L}^{-1}\left[\frac{4B\sqrt{z}(B\sqrt{z}-1)}{(1+B\sqrt{z})^3}\right]=\frac{2}{B\sqrt{\pi}}\frac{1}{t^{3/2}}\int_0^\infty \exp\left(-\frac{u^2}{4t}\right)\left(\frac{u^2}{2t}-1\right) \times\left(u-\frac{u^2}{B}\right)\exp\left(-\frac{u}{B}\right)du = \frac{2B}{\sqrt{\pi}}\frac{1}{t^{3/2}}\int_0^\infty \exp\left(-\frac{B^2y^2}{4t}\right)\left(\frac{y^2B^2}{2t}-1\right) \times(y-y^2)\exp(-y)dy=k(t).$$

The reflection scattering operator is then given by

$$\tilde{R}(t)=[f(t)+k(t)]*g(t). \tag{41}$$

IV. ACOUSTIC PARAMETER SENSITIVITY

In this section, numerical simulations of waves reflected by a slab of porous material are run by varying the independent geometrical parameters of a porous medium described acoustically using the theory developed in the previous sec-

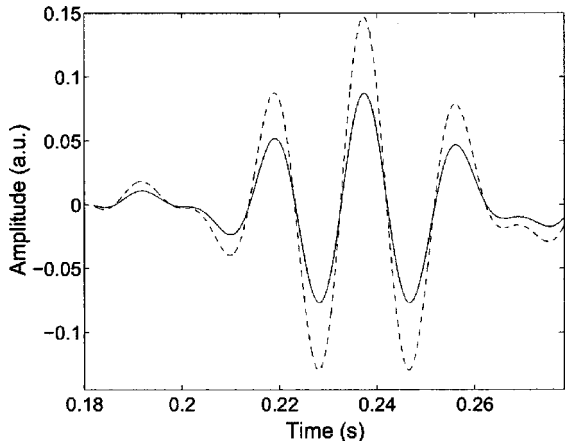

FIG. 2. Incident signal (dashed line) and simulated transmitted signal (solid line).

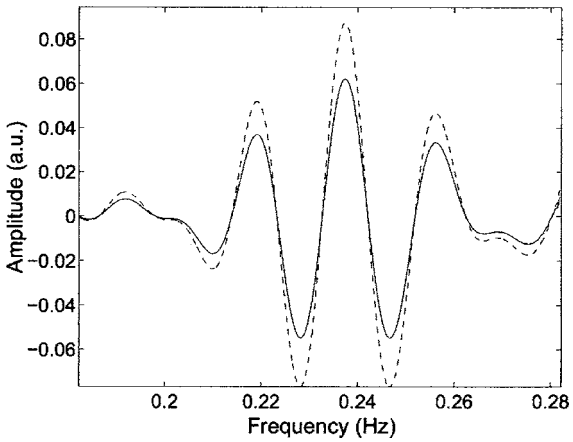

FIG. 4. Comparison between simulated reflected signals corresponding to $\sigma=30\,000$ N m^{-4} s (dashed line) and $\sigma=15\,000$ N m^{-4} s (solid line).

tion. A 50% variation is applied to the governing parameters (flow resistivity σ and porosity ϕ). The numerical values chosen for the physical parameters correspond to quite common acoustic materials as follows: thickness $L=4$ cm, porosity $\phi=0.9$, flow resistivity $\sigma=30\,000$ N m^{-4} s, and radius of the pore $r=70$ μm. The condition of viscous domain (low-frequency approximation) is verified if the frequencies of the incident signal spectrum are much smaller than the characteristic frequency which verify Eq. (4). For this porous sample the characteristic frequency is equal to 1 kHz.

A numerical simulation is produced. The incident signal used in the simulation is given in Fig. 2 (dashed line). The result of the simulation (reflected wave) is a signal as shown in the same figure (Fig. 2) in solid line. Amplitude is given by an arbitrary unit and the point number given in the abscissa is proportional to time. The spectra of the incident and transmitted signals are given in Fig. 3. From Fig. 2, we can see that the reflected wave is just attenuated with no significant dispersion comparing to the incident signal, the two signals have the same spectral bandwidth (Fig. 3).

Figure 4 shows the results obtained after reducing the flow resistivity by 50% of its initial value. The first signal (dashed line) corresponds to the simulated transmitted signal for $\sigma=30\,000$ N m^{-4} s and the second one (solid line) to $\sigma=15\,000$ N m^{-4} s. The values of the other parameters have been kept constant ($L=4$ cm and porosity $\phi=0.9$). The sensitivity of the flow resistivity in reflected mode can be seen for a 50% change. By reducing flow resistivity, the amplitude of reflected wave decreases by 30% of its initial value. This result can be explained by the fact that when flow resistivity decreases, the losses due to the viscous effects become less important in the porous material, the medium is less resistive, and thus the amplitude of the reflected wave decreases.

By reducing the porosity by 50% of its initial value, no change appears in the reflected wave. We can conclude that there is no significant sensitivity to porosity in reflected mode.

From this study, we can gain an insight into the sensitivity of each physical parameter used in this theory. It seems that the flow resistivity is the most important parameter in the description of losses in the viscous domain (low-frequency range). We will try to measure this parameter in the next sections by solving the inverse problem using experimental data of reflected waves.

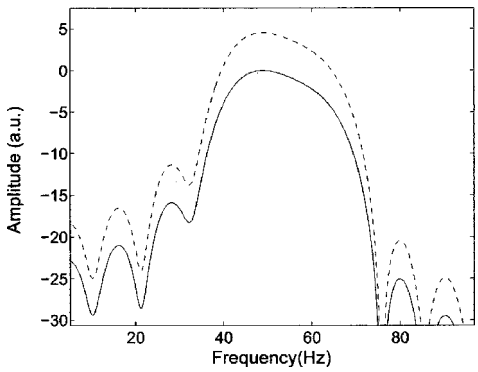

FIG. 3. Spectrum of incident signal (dashed line) and spectrum of transmitted signal (solid line).

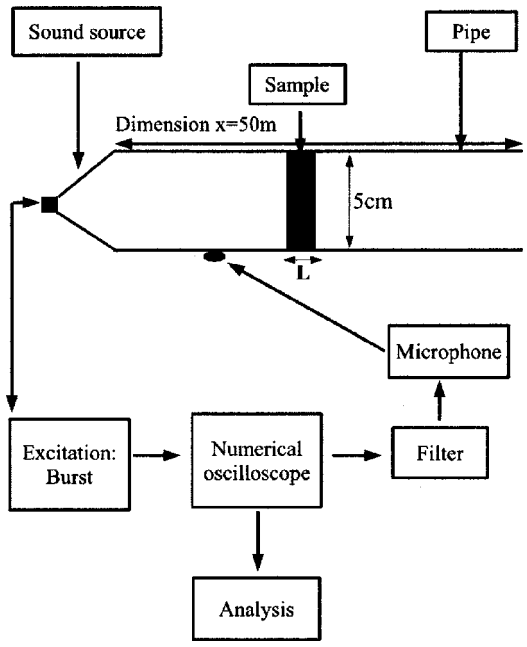

FIG. 5. Experimental setup of acoustic measurements.

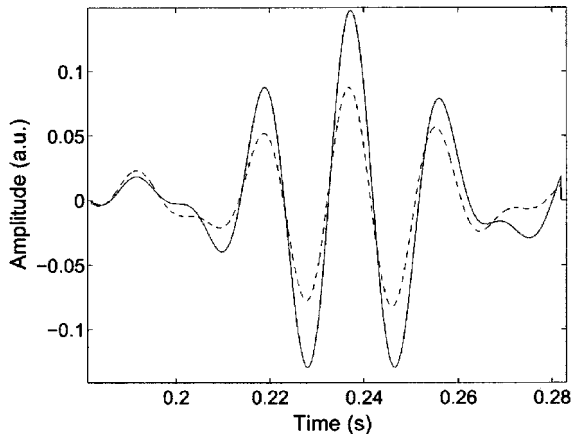

FIG. 6. Experimental incident signal (solid line) and experimental reflected signal (dashed line).

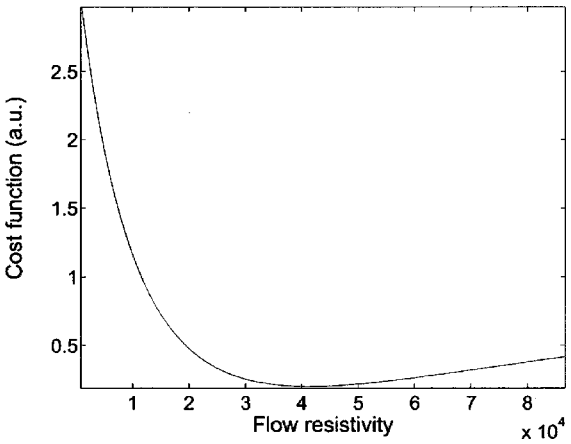

FIG. 8. Variation of the minimization function U with flow resistivity σ.

V. INVERSE PROBLEM

The diffusion of acoustic waves in a slab of porous material in the viscous domain (low frequency) is characterized by two parameters, namely, porosity ϕ and flow resistivity σ, the values of which are crucial for the behavior of sound waves in such materials. It is of some importance to work out new experimental methods and efficient tools for their estimation. The basic inverse problem associated with the slab may be stated as follows: from measurement of the signals reflected outside the slab, find the values of the medium's parameters. The study of the sensitivity of the porosity (in the previous section) shows that this parameter cannot be estimated in reflected mode at low frequencies because of its weak sensitivity. However, the porosity was estimated in reflection at high frequencies.[7,21,25] It has been shown in the previous section that the flow resistivity has a significant sensitivity on reflected waves. We will try to determine σ by solving the inverse problem for waves reflected by the slab of porous material. The inverse problem is to find value for parameter σ which minimizes the function

$$U(\sigma) = \int_0^t [p^r_{\exp,z}(x,t) - p^r(x,t)]^2 dt,$$

where $p^r_{\exp,z}(x,t)$ is the experimentally determined reflected signal and $p^r(x,t)$ is the reflected wave predicted from Eq. (14). However, the analytical method of solving the inverse problem using the conventional least-square method is tedious. In our case, a numerical solution of the least-square method can be found which minimizes $U(\sigma)$ defined by

$$U(\sigma) = \sum_{i=1}^{i=N} [p^r_{\exp,z}(x,t_i) - p^r(x,t_i)]^2, \tag{42}$$

where $p^r_{\exp,z}(x,t_i)_{i=1,2,\ldots N}$ represents the discrete set of values of the experimental reflected signal and $p^r(x,t_i)_{i=1,2,\ldots N}$ is the discrete set of values of the simulated reflected signal. The inverse problem is solved numerically by the least-square method. The next section discusses the solution of the inverse problem based on experimental reflected data.

VI. ACOUSTIC MEASUREMENTS

In application of our model, some numerical simulations are compared with experimental results. To verify the condition of low-frequency range for air-saturated plastic foams having pore radii between 40 and 100 μm, the frequency component of the experimental signals must be very small compared to 1 kHz [Eq. (4)]. Experiments are performed in a guide (pipe) having a diameter of 5 cm and of length 50 m. This length has been chosen for the propagation of transient

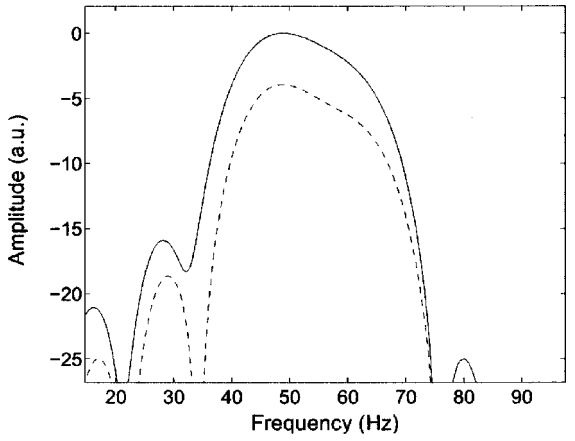

FIG. 7. Spectrum of experimental incident signal (solid line) and of experimental reflected signal (dashed line).

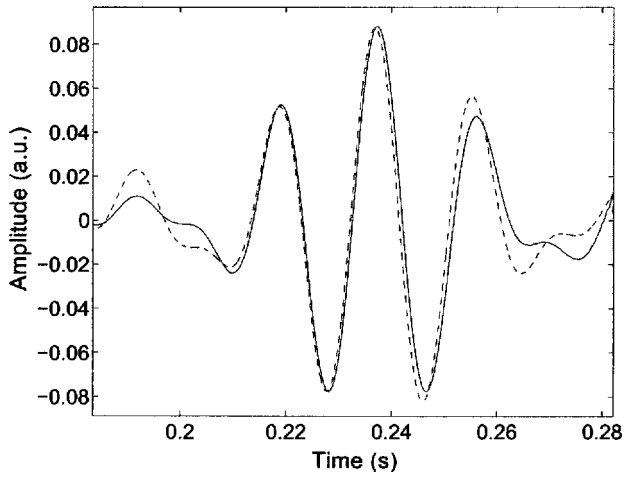

FIG. 9. Comparison between experimental reflected signal (dashed line) and simulated reflected signal (solid line) for the sample M1.

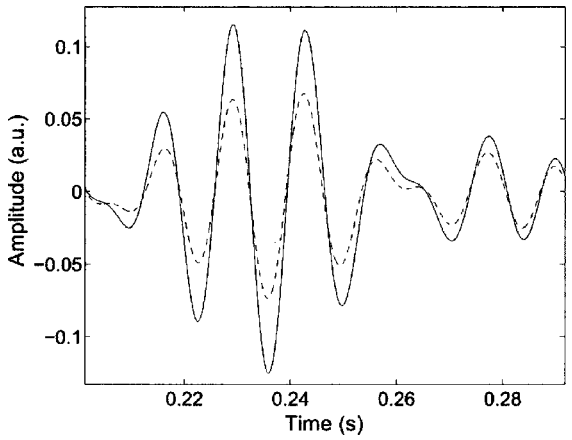

FIG. 10. Experimental incident signal (solid line) and experimental reflected signal (dashed line).

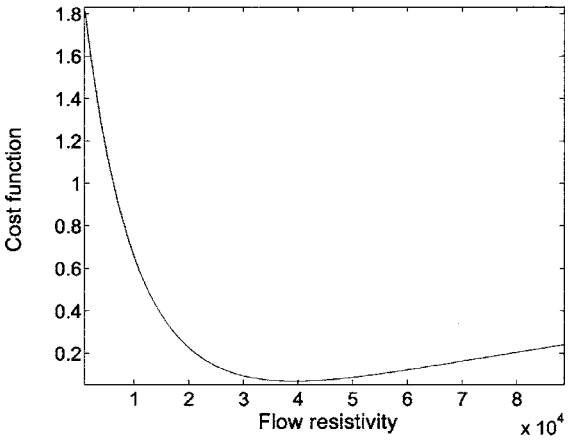

FIG. 12. Variation of the minimization function U with flow resistivity σ.

signals at low frequency. It is not important to keep the pipe straight, it can be rolled in order to save space without perturbations on experimental signals (the cutoff frequency of the tube $f_c \sim 4$ kHz).

A sound source driver unit "brand" constituted by loudspeaker Realistic 40-9000 is used. Bursts are provided by synthesized function generator Standford Research Systems model DS345 30 MHz. The signals are amplified and filtered using model SR 650-Dual channel filter, Standford Research Systems. The signals (incident and reflected) are measured using the same microphone (Bruel & Kjaer, 4190). The incident signal is measured by putting a total reflector in the same position as the porous sample. The experimental setup is shown in Fig. 5.

Consider a cylindrical sample of plastic foam M1 of diameter 5 cm and thickness 3 cm. The flow resistivity of the sample M1 was measured using the method of Bies and Hansen,[9] given the value $\sigma = 40\,000 \pm 6000$ N m^{-4} s. Figure 6 shows the experimental incident signal (solid line) generated by the loudspeaker in the frequency bandwidth of 35–75 Hz and the experimental reflected signal (dashed line). Figure 7 shows the spectra of the two signals. From the spectra of the two signals, the reader can see that they have practically the same bandwidth which means that there is no dispersion. After solving the inverse problem numerically for the flow resistivity, we find the following optimized value: $\sigma = 40\,500 \pm 2000$ N m^{-4} s. We present in Fig. 8 the variation of the minimization function U given in Eq. (42) with the flow resistivity σ. In Fig. 9, we show a comparison between an experimental reflected signal and a simulated reflected signal for the optimized value of the flow resistivity. The difference between the two curves is slight, which leads us to conclude that the optimized value of the flow resistivity is good.

Let us now solve the inverse problem for the same sample M1 in the frequency bandwidth of 45–100 Hz. The experimental incident signal generated by the loudspeaker (solid line) and the reflected one (dashed line) are given in Fig. 10. Their spectra are given in Fig. 11; we can see in this case that the center frequency of the signal is 70 Hz. By solving the inverse problem and minimizing the cost function U (see Fig. 12), we obtain the following optimized value of the flow resistivity: $\sigma = 39\,500 \pm 2000$ N m^{-4} s. Figure 13 shows a comparison between an experimental reflected signal and a simulated signal obtained by optimization from the inverse problem. Here, again, the correlation of theoretical prediction and experimental data is good. This study has been carried on, in the frequency bandwidth of 80–140 Hz and have also given good results ($\sigma = 41\,500 \pm 2000$ N m^{-4} s). It can be seen that for the different

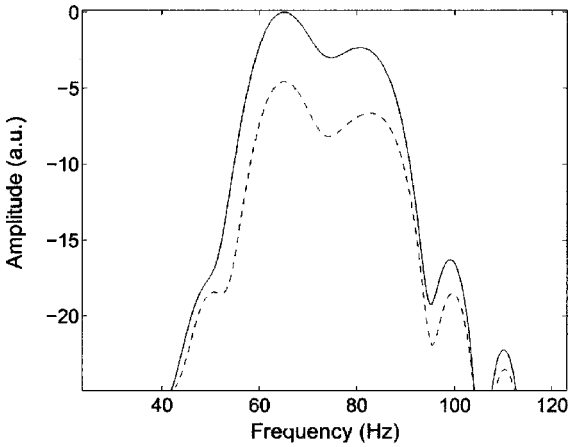

FIG. 11. Spectrum of experimental incident signal (solid line) and of experimental reflected signal (dashed line).

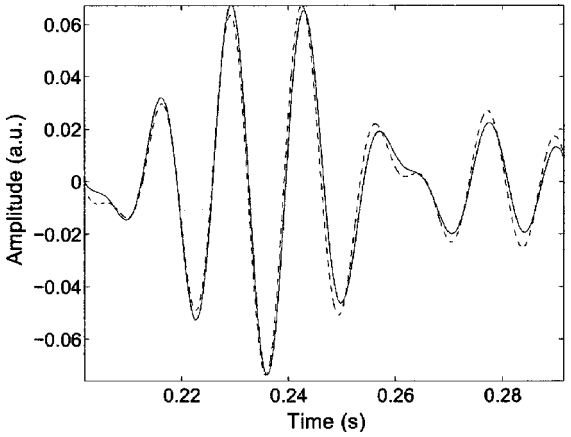

FIG. 13. Comparison between experimental reflected signal (dashed line) and simulated reflected signal (solid line) for the sample M1.

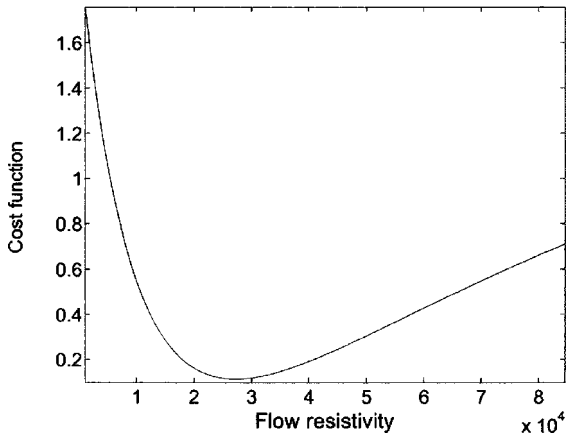

FIG. 14. Variation of the minimization function U with flow resistivity σ for the sample M2 in the frequency bandwidth of 35–70 Hz

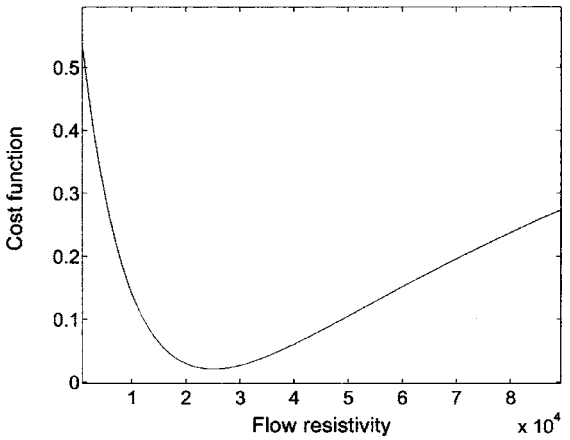

FIG. 16. Variation of the minimization function U with flow resistivity σ for the sample M2 in the frequency bandwidth of 70–130 Hz

frequency bandwidths of the experimental incident signals, the optimized values obtained using this method are close to those produced using classical methods (Bies and Hansen[9]).

Let us consider another sample M2 less resistive, of diameter 5 cm and thickness 2.66 cm. The flow resistivity of the sample M2 was measured using the method of Bies and Hansen,[9] given the value $\sigma=26\,000\pm6000$ N m^{-4} s. Different frequency bandwidths have been investigated between 40 and 130 Hz. By solving the inverse problem for the flow resistivity and minimizing the cost function U given by Eq. (46), we show the results of the inverse problem in Figs. 14–16. The obtained optimized values of the flow resistivity and viscous permeability are $\sigma_1=27\,000\pm2000$ N m^{-4} s, $\sigma_2=25\,000\pm2000$ N m^{-4} s, and $\sigma_3=25\,000\pm2000$ N m^{-4} s. The reader can see the slight difference between the optimized values of the flow resistivity obtained with this method and the other classical method (Bies and Hansen[9]). Using these optimized values, we compare the simulated transmitted signals and experimental signals. The results of the comparison are shown in Figs. 17–19. The correspondence between experiment and theory is good, which leads us to conclude that this method based on the solution of the inverse problem is appropriate for estimating the flow resistivity of porous materials with rigid frame.

VII. CONCLUSION

In this article, an inverse scattering estimate of the flow resistivity was given by solving the inverse problem for waves reflected by a slab of air-saturated porous material. The inverse problem is solved numerically by the least-square method. The reconstructed values of flow resistivity is close to those using classical methods. This method is an alternative to the usual methods (Bies and Hansen[9]) that involves the use of techniques for measuring the flow rate of fluids and pressure differences.

The direct problem is based upon the diffusion equation in the time domain in a slab of porous material in the viscous domain (low-frequency range). The interaction of the sound pulse with the fluid-saturated porous material was described by a time domain equivalent fluid model.

The sensitivity of the porosity and flow resistivity was studied and it showed their effect on the reflected wave by the material. This study has demonstrated that reflection is much more sensitive to flow resistivity than to porosity, the effect of the porosity in reflected mode is negligible as it has been observed in transmission mode in the asymptotic domain[7] (high-frequency range).

We hope, in the future, to extend this method to porous

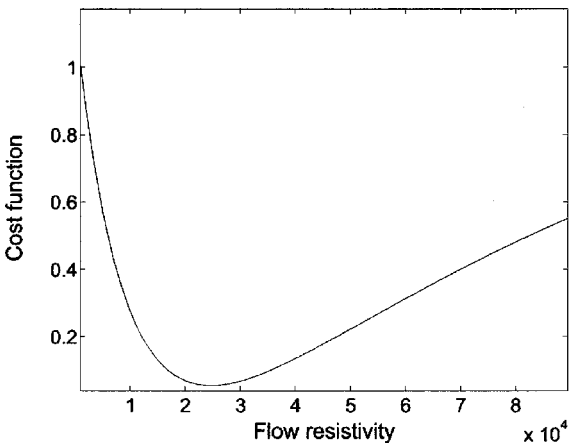

FIG. 15. Variation of the minimization function U with flow resistivity σ for the sample M2 in the frequency bandwidth of 45–95 Hz

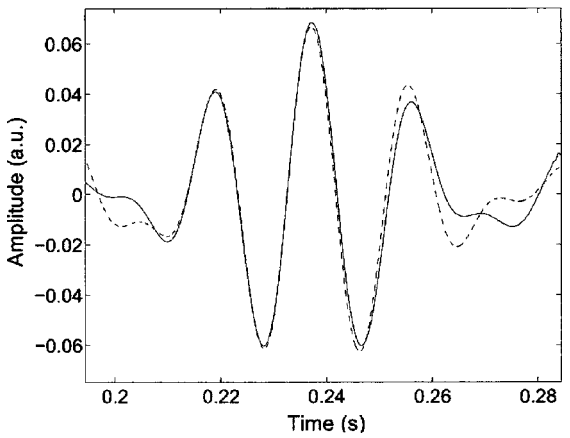

FIG. 17. Comparison between experimental reflected signal (dashed line) and simulated reflected signal (solid line) for the sample M2 in the frequency bandwidth of 35–70 Hz.

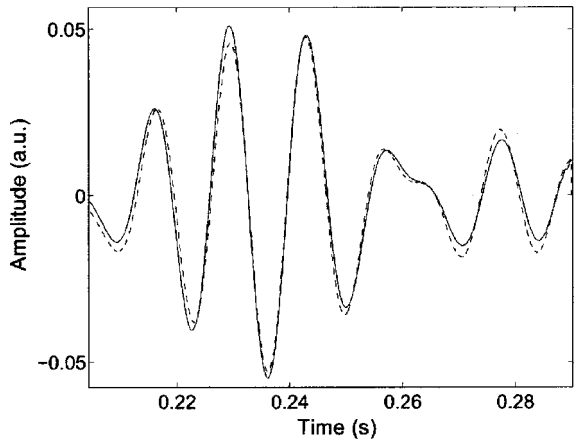

FIG. 18. Comparison between experimental reflected signal (dashed line) and simulated reflected signal (solid line) for the sample M2 in the frequency bandwidth of 45–95 Hz.

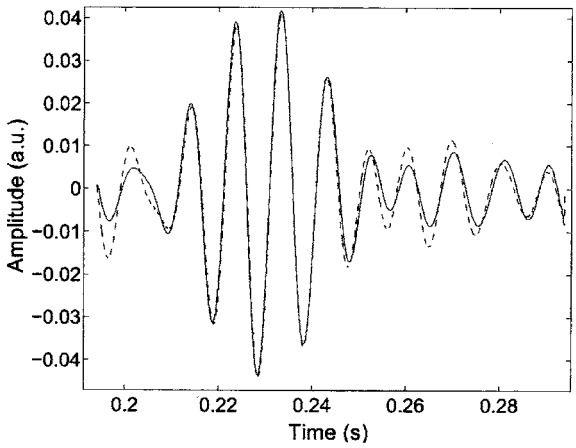

FIG. 19. Comparison between experimental reflected signal (dashed line) and simulated reflected signal (solid line) for the sample M2 in the frequency bandwidth of 70–130 Hz.

media with elastic frame, such as cancellous bone saturated with viscous fluid, in order to estimate other parameters which play an important role in acoustic propagation. The advantage of the data concept using diffusive wave is its simple analysis and similarity to the propagative wave concept which, however, is more complicated. The diffusive wave at low frequency is not subjected to the dispersion but is simply attenuated, its frequency and temporal bandwidth are the same as the incident signal, and experimental detection of it is easy for resistive media compared to propagative transmitted wave in the asymptotic domain (high-frequency range).

APPENDIX: EXPRESSION OF THE REFLECTION AND TRANSMISSION COEFFICIENTS

After developing [in Eq. (37)] the hyperbolic sine and cosine functions in exponential series, we obtain the following expressions of the reflection coefficient $R(z)$:

$$R(z) = \frac{(1-B^2 z)[\exp(L\sqrt{Dz}) - \exp(-L\sqrt{Dz})]}{(1+B\sqrt{z})^2 \exp(L\sqrt{Dz}) - (1-B\sqrt{z})^2 \exp(-L\sqrt{Dz})}$$

$$= \frac{1-B\sqrt{z}}{1+B\sqrt{z}}[1-\exp(-2L\sqrt{Dz})] \times \frac{1}{1-[(1-B\sqrt{z})/(1+B\sqrt{z})]^2 \exp(-2L\sqrt{Dz})}$$

$$= \frac{1-B\sqrt{z}}{1+B\sqrt{z}}[1-\exp(-2L\sqrt{Dz})] \sum_{n\geq 0} \left(\frac{1-B\sqrt{z}}{1+B\sqrt{z}}\right)^{2n} \times \exp(-2nL\sqrt{Dz}).$$

Finally, we obtain the expression of the reflection coefficient taking into account the n-multiple reflections in the material,

$$R(z) = \frac{1-B\sqrt{z}}{1+B\sqrt{z}} \sum_{n\geq 0} \left(\frac{1-B\sqrt{z}}{1+B\sqrt{z}}\right)^{2n} [\exp(-2nL\sqrt{Dz}) - \exp(-2(n+1)L\sqrt{Dz})].$$

[1] J. F. Allard, *Propagation of Sound in Porous Media: Modeling Sound Absorbing Materials* (Chapman and Hall, London, 1993).
[2] P. Leclaire, L. Kelders, W. Lauriks, C. Glorieux, and J. Thoen, J. Acoust. Soc. Am. **99**, 1944 (1996).
[3] Z. E. A. Fellah and C. Depollier, J. Acoust. Soc. Am. **107**, 683 (2000).
[4] P. B. Nagy, L. Adler, and B. P. Bonner, Appl. Phys. Lett. **56**, 2504 (1990).
[5] P. B. Nagy, J. Acoust. Soc. Am. **93**, 3224 (1993).
[6] *Inverse Problems in Mathematical Physics*, edited by L. Päivärinta and E. Somersalo (Springer, Berlin, 1993).
[7] Z. E. A. Fellah, C. Depollier, S. Berger, W. Lauriks, P. Trompette, and J. Y. Chapelon, J. Acoust. Soc. Am. **114**, 2561 (2003).
[8] M. E. Delany and E. N. Bazley, Appl. Acoust. **3**, 105 (1970).
[9] D. A. Bies and C. H. Hansen, Appl. Acoust. **13**, 357 (1980).
[10] T. F. W. Embleton, J. E. Piercy, and G. A. Daigle, J. Acoust. Soc. Am. **74**, 1239 (1983).
[11] R. L. Brown and R. H. Bolt, J. Acoust. Soc. Am. **13**, 337 (1942).
[12] R. W. Leonard, J. Acoust. Soc. Am. **17**, 240 (1946).
[13] M. R. Stinson and G. A. Daigle, J. Acoust. Soc. Am. **83**, 2422 (1988).
[14] P. M. Morse, R. H. Bolt, and R. L. Brown, J. Acoust. Soc. Am. **12**, 475 (1941).
[15] R. N. Chandler, J. Acoust. Soc. Am. **70**, 116 (1981).
[16] R. N. Chandler and D. L. Johnson, J. Appl. Phys. **52**, 3391 (1981).
[17] *Fluid Mechanics Measurements*, edited by R. J. Goldstein (Hemisphere, New York, 1983).
[18] A. Gemant, J. Appl. Phys. **12**, 725 (1941).
[19] D. L. Johnson, J. Koplik, and R. Dashen, J. Fluid Mech. **176**, 379 (1987).
[20] M. A. Biot, J. Acoust. Soc. Am. **28**, 168 (1956).
[21] Z. E. A. Fellah, F. G. Mitri, C. Depollier, S. Berger, W. Lauriks, and J. Y. Chapelon, J. Appl. Phys. **94**, 7914 (2003).
[22] D. Lafarge, P. Lemarnier, J. F. Allard, and V. Tarnow, J. Acoust. Soc. Am. **4**, 1995 (1996).
[23] D. L. Johnson, Proceedings of the International School of Physics Enrico Fermi, Course XCIII, edited by D. Sette, North Holland, Amsterdam, 1986 (unpublished), p. 255.
[24] I. S. Gradshteyn and I. M. Ryzhik, *Table of Integrals, Series, and Products*, 4th ed. (Academic, New York, 1965).
[25] O. Umnova, K. Attenborough, H.-C. Shin, and A. Cummings, Appl. Acoust. **66**, 607 (2005).